Eur. Phys. J. A **23**, 491–499 (2005)
DOI 10.1140/epja/i2004-10094-8

THE EUROPEAN PHYSICAL JOURNAL A

Analysis of Θ^+ production in K^+-Xe collisions

A. Sibirtsev[1], J. Haidenbauer[1], S. Krewald[1], and Ulf-G. Meißner[1,2,a]

[1] Institut für Kernphysik (Theorie), Forschungszentrum Jülich, D-52425 Jülich, Germany
[2] Helmholtz-Institut für Strahlen- und Kernphysik (Theorie), Universität Bonn, Nußallee 14-16, D-53115 Bonn, Germany

Received: 8 July 2004 / Revised version: 22 September 2004 /
Published online: 17 January 2005 –
Communicated by Th. Walcher

Abstract. The reaction $K^+\mathrm{Xe} \to K^0pX$ is investigated in a meson-exchange model including rescattering of the secondary protons with the aim to analyze the evidence for the $\Theta^+(1540)$-resonance reported by the DIANA Collaboration. We confirm that the kinematical cuts introduced by the DIANA Collaboration efficiently suppress the background to the $K^+n \to K^0p$ reaction which may contribute to the $\Theta^+(1540)$ production. We find that these kinematical cuts do not produce a narrow structure in the K^0p effective-mass spectra near 1540 MeV. We study the effect of a narrow Θ^+-resonance of both positive and negative parity in comparison with the DIANA data. We show that the $K^+\mathrm{Xe} \to K^0pX$ calculations without Θ^+ contribution as well as the results obtained with a Θ^+ width of 1 MeV are in comparably good agreement with the DIANA results. More dedicated experiments are called for to establish this exotic baryon resonance.

PACS. 11.80.-m Relativistic scattering theory – 13.60.Le Meson production – 13.75.Jz Kaon-baryon interactions – 25.80.Nv Kaon-induced reactions

1 Introduction

The evidence for a narrow $S = +1$ baryon resonance in photoproduction from the neutron reported in ref. [1] and the subsequent observation of such a structure in the invariant-mass spectrum of the kaon-nucleon (KN) system in other reactions led to a wealth of theoretical investigations dealing with this topic. By now the production of this exotic baryon state, called $\Theta^+(1540)$, in basically every elementary photo-, kaon- or nucleon-induced process has been worked out in detail assuming positive as well as negative parity for the Θ^+ state. It is interesting, however, that so far —to the best of our knowledge— there is not a single calculation that tries to provide a theoretical description of any of those experiments where the Θ^+ baryon resonance was actually detected. Certainly, one has to concede that in several of the works where evidence for the Θ^+ was claimed, cuts are applied which are not described in much detail and therefore a direct and quantitative comparison of any model calculation with those data would be difficult if not impossible. Luckily, there are also exceptions and one of them is the result of the DIANA Collaboration [2], where the Θ^+-resonance was observed in K^+ collisions with Xe nuclei.

In this paper we present a detailed and microscopic calculation of the K^0p effective-mass spectrum for the charge-exchange reaction $K^+\mathrm{Xe} \to K^0pX$. We aim at a quantitative analysis of the mass spectrum that was published by the DIANA Collaboration [2]. The main ingredient of our calculation is an elementary KN scattering amplitude that is taken from the meson-exchange model developed by the Jülich group [3,4]. The role and significance of the $\Theta^+(1540)$ for a quantitative description of the DIANA data are investigated by employing variants of the Jülich KN model where a Θ^+-resonance with different widths was included consistently [5,6]. Since the parity of the Θ^+-resonance is not yet known we consider here the cases of positive as well as negative parity. We assume this exotic resonance to have spin 1/2 throughout.

The paper is structured in the following way. In the subsequent section we provide a short description of the KN interaction model of the Jülich group. We also explain how the Θ^+-resonance is implemented into the model. Furthermore we point to the importance of unitarity and emphasize the interplay between the background phase, provided by the non-pole part of the interaction, and the resonance structure. This feature plays a decisive role in our analysis of the DIANA data. In sect. 3 first we describe how the calculations of the K^0p effective-mass spectrum for the charge-exchange reaction $K^+\mathrm{Xe} \to K^0pX$ are performed. Then we present a detailed quantitative comparison of our model calculation with the data of the DIANA Collaboration, considering their results before cuts were applied as well as those with cuts. The paper ends with a short summary.

[a] e-mail: meissner@itkp.uni-bonn.de

2 The kaon-nucleon amplitude

We use the Jülich meson-exchange model for the KN interaction. A detailed description of this model is given in refs. [3,4]. It was constructed along the lines of the full Bonn NN model [7] and its extension to the hyperon-nucleon YN system [8]. Specifically, this means that one has used the same scheme (time-ordered perturbation theory) and the same type of processes. Moreover, most of the vertex parameters (coupling constants and cut-off masses of the vertex form factors) appearing in the diagrams that contribute to the interaction potential V, cf. fig. 1 of ref. [4], have been fixed already by the study of other reactions.

Once the KN interaction potential V is derived, the corresponding reaction amplitude T is then obtained by solving a Lippmann-Schwinger equation defined by the time-ordered perturbation theory,

$$T = V + VG_0T \ , \tag{1}$$

where G_0 is the free propagator. Taking the solution of such a scattering equation implies that the resulting reaction amplitude T automatically fulfils the requirements of (two-body) unitarity. In the present investigation we use the KN model (I) described in ref. [4]. Results for phase shifts and also for differential cross-sections and polarizations can be found in ref. [4]. Evidently this model yields a good overall reproduction of all presently available empirical information on KN scattering. Specifically, it describes the data up to kaon laboratory momenta of $p_K \approx 1$ GeV/c, *i.e.* well beyond the region of the observed Θ^+-resonance structure which corresponds to the momentum $p_K \simeq 440$ MeV/c.

The Θ^+-resonance is included in the model by adding a pole diagram with a bare mass $\hat{M}_{\Theta^+}$ and a bare coupling constant $\hat{g}_{KN\Theta^+}$ to the other diagrams that contribute to V, cf. ref. [5] for details. When this interaction is then iterated in the Lippmann-Schwinger equation, the $KN\Theta^+$ vertex gets dressed by the non-pole part of the interaction and the Θ^+ acquires a width and also its physical mass via self-energy loops. Note that the bare mass and bare coupling constant are free parameters that are adjusted to obtain the desired physical mass and width of the Θ^+-resonance. The latter are adopted to be $M_{\Theta^+} = 1540$ MeV and, for exploratory purposes, $\Gamma_{\Theta^+} = 1, 5,$ and 10 MeV.

Depending on the parity of the Θ^+ the resonance will contribute to different partial waves of the KN interaction. If the Θ^+ is a $J^P = \frac{1}{2}^+$ state, as predicted by, *e.g.*, the chiral quark-soliton model, then it couples to the P_{01} channel (we use the standard spectroscopic notation $L_{I\,2J}$). If Θ has the opposite parity it will occur in the S_{01} partial wave. The phase shifts in these two partial waves exhibit quite different characteristics as can be seen in fig. 1. The S_{01} phase shift is small and basically repulsive. In fact $\delta_{S_{01}}$ is practically zero up to the momentum of $p_K = 440$ MeV/c corresponding to the Θ^+-resonance mass, cf. fig. 2. In contrast, the P_{01} phase shift is large and attractive. As a consequence, the total KN cross-section

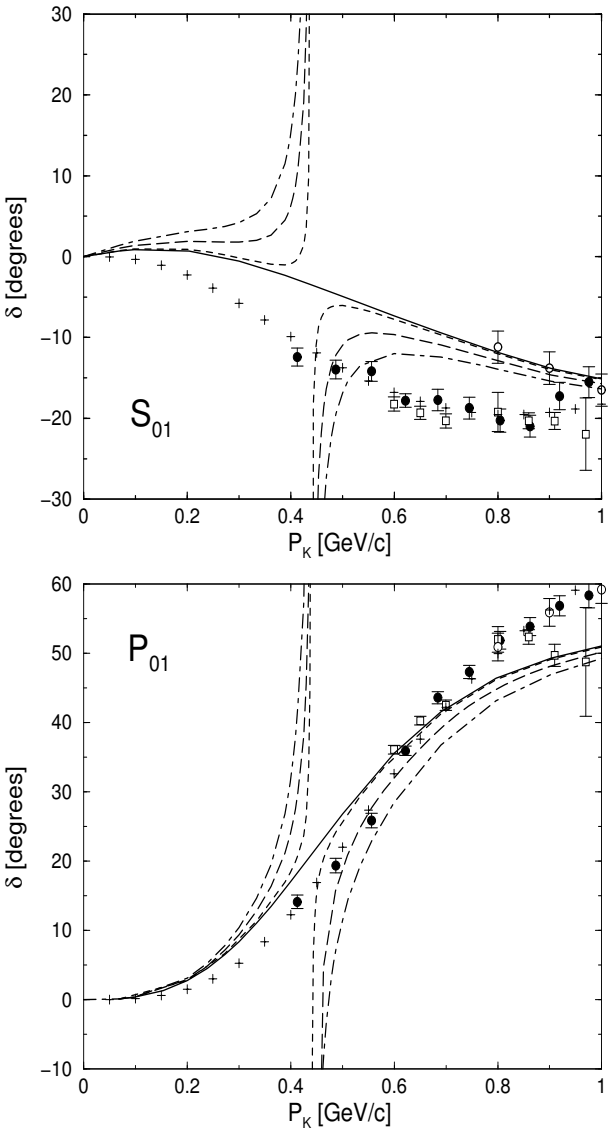

Fig. 1. The S_{01} and P_{01} phase shifts for KN scattering as a function of the kaon momentum. The solid lines show the calculations without Θ^+ contribution. The short-dashed line is our calculation with $\Gamma_{\Theta^+} = 1$ MeV, the long-dashed line corresponds to $\Gamma_{\Theta^+} = 5$ MeV and the dash-dotted line to $\Gamma_{\Theta^+} = 10$ MeV. Note that the phases for the resonance cases are shown modulo π.

for isospin $I = 0$ is dominated by the P_{01} partial wave, while the contribution of the S_{01} partial wave is roughly given by the result on the very left side of fig. 2.

Adding a resonance in these two partial waves generates again quite different characteristics. In the S_{01} partial wave we obtain basically a Breit-Wigner–type structure because the non-resonant background is rather small. In the P_{01} partial wave, on the other hand, there is an interference of the background phase with the added resonance structure. In particular, the phase will not only rise beyond 90° (because of the resonance) but even beyond 180° (because of the large background). For momenta around

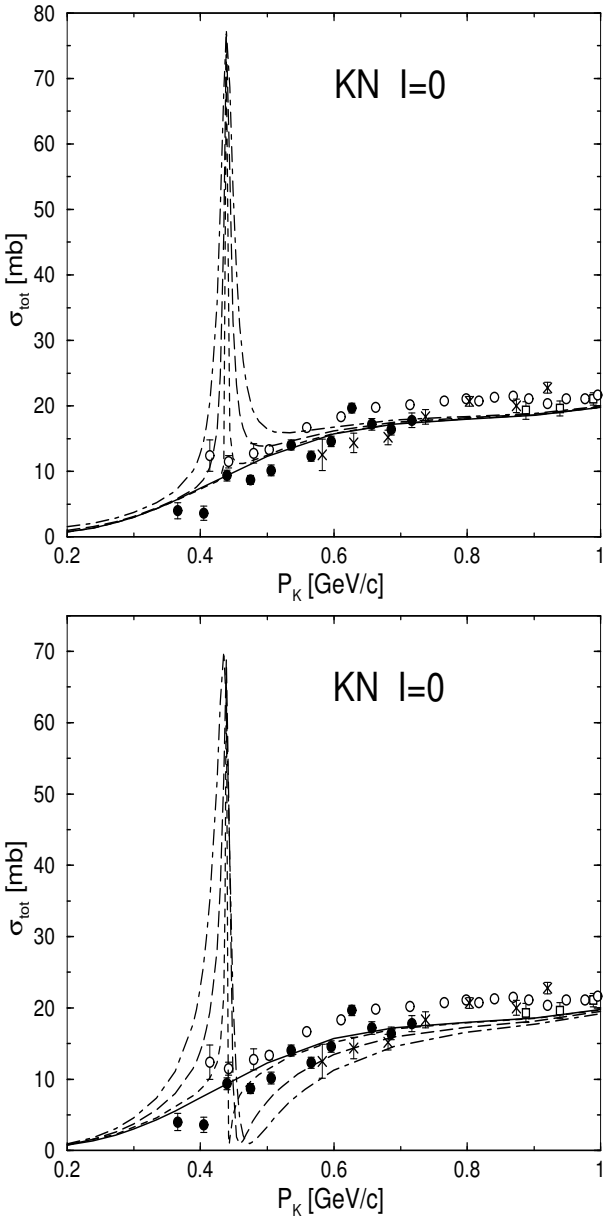

Fig. 2. The KN reaction cross-section for the $I = 0$ channel as a function of the kaon momentum. Results are shown for negative (top) and positive (bottom) parity of the Θ^+-resonance. The various curves correspond to different Θ^+ widths, $\Gamma_{\Theta^+} =$ 1 MeV (short-dashed line), 5 MeV (long-dashed line), and 10 MeV (dash-dotted line), while the solid line is the prediction without a Θ^+ contribution. Data are taken from refs. [9] (filled circles), [10] (squares), [11] (open circles), and [12] (crosses).

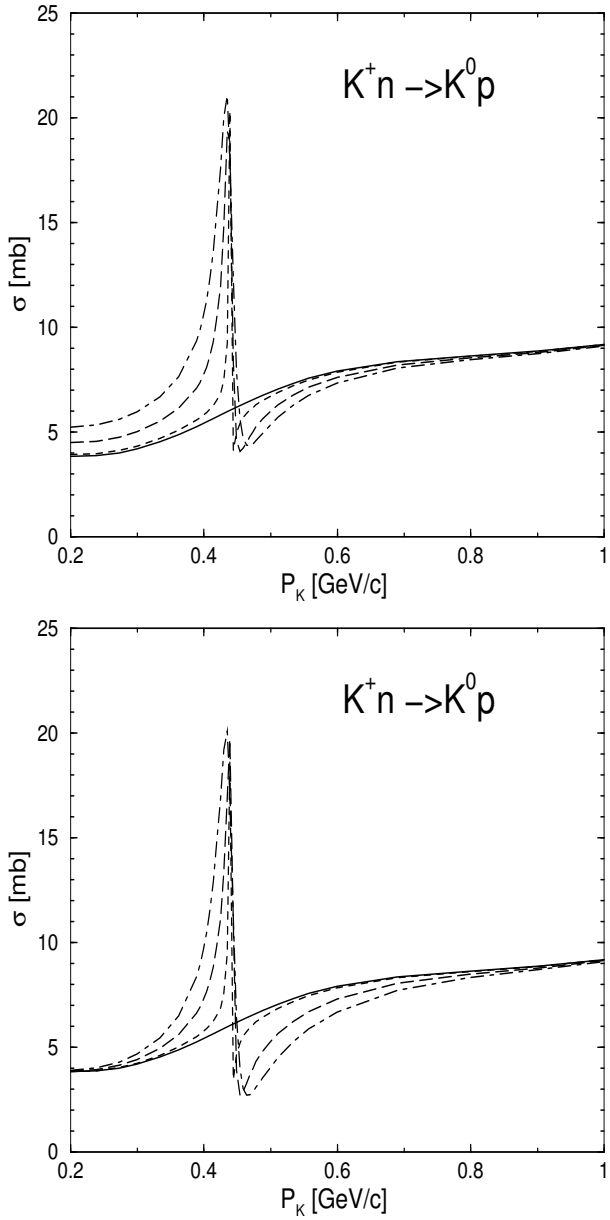

Fig. 3. The $K^+n \to K^0p$ reaction cross-section as a function of the kaon momentum. For notations, see fig. 2.

the region where the phase shift passes through 180° there will be practically no contribution of this partial wave to the total cross-section because $\sigma_L \propto \sin^2(\delta_L)$. As a consequence, a resonance in the P_{01} partial wave causes a rather striking bump-dip structure in the KN $I = 0$ cross-section, cf. fig. 2.

Figure 3 shows the cross-section for the charge-exchange reaction $K^+n \to K^0p$ as a function of the kaon momentum. This is the elementary process that is needed for analyzing the reaction $K^+\mathrm{Xe} \to K^0pX$ measured by the DIANA Collaboration. Obviously, here the characteristic differences between the S_{01} and P_{01} resonances have basically disappeared. Since the charge-exchange amplitude is given by the difference of the isospin $I = 1$ and $I = 0$ amplitudes we now get an interference of the (larger) S_{11} partial wave with the resonant S_{01} partial wave and that leads to a similar bump-dip structure in the cross-section as produced by the interference of the resonance with the background in the P_{01} case. Still one can see that for the negative-parity case the dip after the resonance energy is somewhat less pronounced, cf. the two cases in fig. 3.

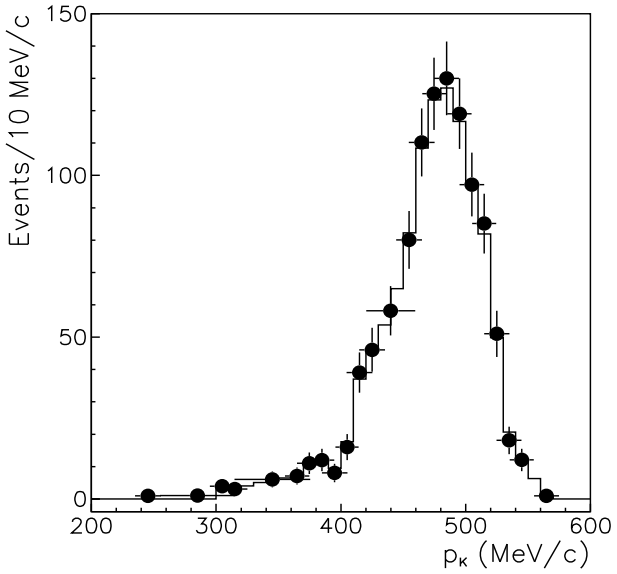

Fig. 4. The momentum spectrum of the incident K^+-mesons. The circles show experimental results, while the histogram is our simulation.

This behaviour of the elementary KN and $K^+n \to K^0p$ cross-sections should be also reflected in all of those reactions where the Θ^+ was observed because there again the complete KN amplitude enters. In the next section we examine in detail the influence of these characteristic features induced by the presence of a Θ^+-resonance on the K^0p mass spectrum for the reaction $K^+\mathrm{Xe} \to K^0pX$ measured by the DIANA Collaboration.

We would like to mention that there are no data on the elementary $K^+n \to K^0p$ process. However, the charge-exchange channel has been measured on a deuteron target, *i.e.* in the reaction $K^+d \to K^0pp$. In ref. [6] we have investigated this reaction employing the Jülich KN model (I), that is used also in the present work, and we have found that the model predictions are in very good agreement with corresponding data.

3 The $K^+Xe \to K^0pX$ model

There are some specific aspects of the DIANA experiment that substantially constrain our model calculations. The incident K^+-mesons have no fixed momentum but are distributed between (roughly) 300 and 550 MeV/c as is shown by fig. 4. Because of the reaction kinematics kaons with that spectrum would produce a K^0p mass distribution, which is obviously enhanced at large masses. In addition the free $K^+n \to K^0p$ reaction cross-section increases by a factor 2.5 within the range $300 \le p_K \le 550$ MeV/c, as is illustrated in fig. 3. Therefore, it is natural to expect that the observed K^0p mass spectrum should be shifted towards the maximal available K^0p mass.

The measured K^0p mass spectrum shows an absolutely different shape as is indicated by fig. 5. Prior to kinematical cuts the DIANA data show an enhancement at low K^0p masses. This can be understood in terms of nuclear

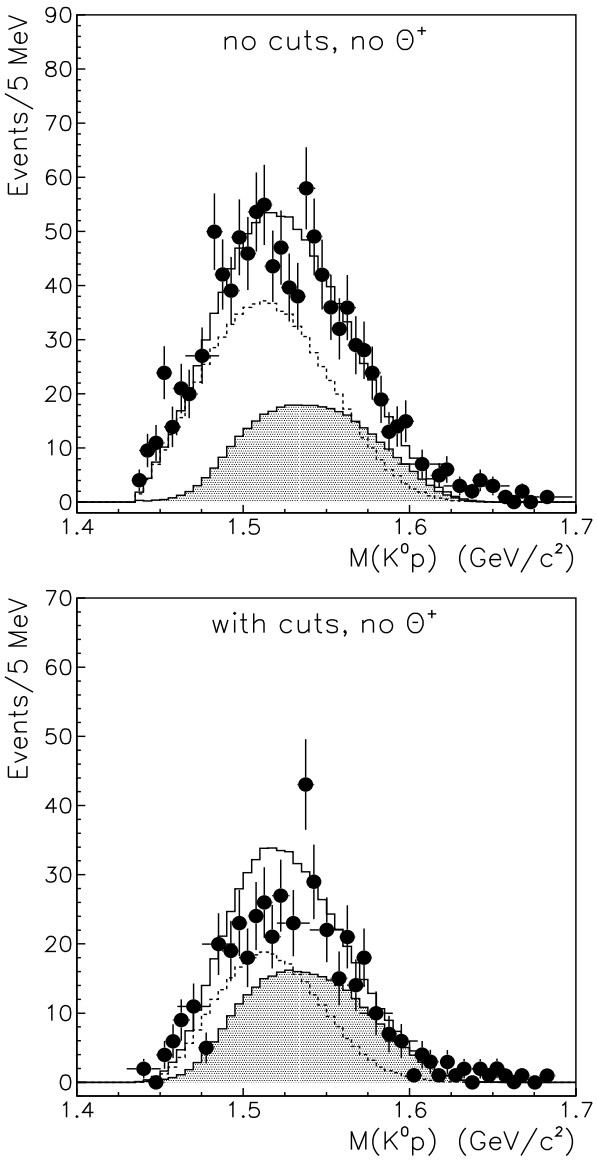

Fig. 5. The K^0p invariant-mass spectrum from the K^+Xe reaction. The circles show experimental results from the DIANA Collaboration [2] without (top) and with kinematical cuts (bottom). The histograms are our results without the inclusion of a Θ^+-resonance, with and without experimental cuts. Shaded histograms show the spectrum from direct $K^+n \to K^0p$ production on a bound target neutron, for the dashed curve an additional single rescattering of the proton was taken into account, while the solid curve is their sum.

effects. As will be shown later, the enhancement for low masses comes from the nuclear rescattering of the final protons or K^0-mesons. Through the rescattering in the nucleus the particle transfers part of its initial momentum to the target nucleon by an elastic or inelastic scattering. Therefore one should model not only the $K^+n \to K^0p$ reaction in Xe, but also the rescattering of the proton and the kaon.

It is clear that the reaction $K^+N \to K^+N$ with N being either a bound proton or neutron can also contribute.

Then the final K^+ might interact with a neutron to be converted to a K^0. However, the kaon mean free path $\lambda_K \simeq 5$ fm is quite large and thus the probability of kaon rescattering in the final nucleus is smaller compared to the rescattering of the final proton which has $\lambda_p \simeq 1.5$ fm. Here we do not consider the final-state interaction of the kaon.

Another feature of the DIANA experiment is the availability of the measured K^0p mass spectrum prior and after the kinematical cuts. These cuts were used for attenuation of the background from nuclear rescattering. In our calculations we are comparing to the data with and without kinematical cuts in order to control the contribution from the direct $K^+n \to K^0p$ reaction in the Xe nucleus and the rescattering processes.

We evaluate the differential $K^+n \to K^0p$ cross-section on a bound neutron from

$$\frac{\mathrm{d}^3\sigma}{\mathrm{d}p\mathrm{d}\Omega} = \int \Phi(p_K)\mathrm{d}p_K \times \int P(E_q,q)|T_{KN}(s_{KN},\Omega)|^2\mathrm{d}E_q\mathrm{d}^3q\,, \quad (2)$$

where $\Phi(p_K)$ is the K^+-meson spectrum shown in fig. 4 and T_{KN} is the amplitude for the reaction $K^+n \to K^0p$, which depends on the K^0-meson production angle Ω and the squared invariant energy of the incident kaon and target neutron given by

$$s_{KN} = (E_K + E_q)^2 - (\boldsymbol{p}_K + \boldsymbol{q})^2. \quad (3)$$

Note that to evaluate eq. (2) we utilize the on-shell amplitude, which should be a reasonable approximation at low kaon momenta.

The nuclear spectral function $P(E_q,q)$ defines the joint probability to find in a nucleus a nucleon with momentum q and total energy E_q. It is clear that the relation between q and E_q in nuclei is not given by the free dispersion relation. Within the Thomas-Fermi approximation the spectral function is given as

$$P(E_q,q) = \frac{3}{4\pi q_{\mathrm{F}}^{3/2}}\Theta(q_{\mathrm{F}} - |\boldsymbol{q}|) \times\delta\left(E_q - \sqrt{q^2+m_N^2} - U(q,\rho)\right), \quad (4)$$

where q_{F} is the Fermi momentum, m_N is the free nucleon mass and the nuclear potential U depends on the nucleon momentum q and on the density ρ as [13,14]

$$U(q,\rho) = A_1\frac{\rho}{\rho_0} + B_1\left(\frac{\rho}{\rho_0}\right)^{1.24} + \frac{2\pi C_1\Lambda_1}{\rho_0} \times\left[\frac{q_{\mathrm{F}}^2+\Lambda_1^2-q^2}{2q\Lambda_1}\times\ln\frac{(q+q_{\mathrm{F}})^2+\Lambda_1^2}{(q-q_{\mathrm{F}})^2+\Lambda_1^2} + \frac{2q_{\mathrm{F}}}{\Lambda_1} - 2\left(\arctan\frac{q+q_{\mathrm{F}}}{\Lambda_1} - \arctan\frac{q-q_{\mathrm{F}}}{\Lambda_1}\right)\right], \quad (5)$$

where $A_1 = -110.44$ MeV, $B_1 = 140.9$ MeV, $C_1 = -64.95$ MeV and $\Lambda_1 = 1.58q_{\mathrm{F}}$. Furthermore, for the calculations with the uncorrelated part of the momentum distribution for the finite nuclei we use $q_{\mathrm{F}} = 220$ MeV/c [15,16].

We neglect the high momentum or correlated part of the spectral function, which contributes to subthreshold particle production [17,18], but does not affect the results of the present study. Indeed the maximum of the spectral function for high momenta, which is attributed to short-range and tensor correlations, corresponds to a total energy of the bound nucleon given as [16,17],

$$E_q \simeq m_N - 2\epsilon - \frac{q^2}{2m_N}, \quad (6)$$

with $\epsilon \simeq 7$ MeV. By inserting this energy E_q into eq. (3) one may show that the high-momentum component of the spectral function would not distort noticeably the K^0p invariant-mass spectrum.

Note that for the total nuclear momentum distribution the Fermi momentum for the ^{131}Xe nucleus is $q_{\mathrm{F}} \simeq 265$ MeV/c and the corresponding average nucleon separation energy is roughly -42 MeV [15], which is substantially beyond the applicability of the Thomas-Fermi approximation. In order to include into the calculations the high-momentum tail of the nuclear momentum distribution one needs to use a realistic spectral function or to explore the dispersion relation given by eq. (6).

However, as was shown in ref. [18] calculations within the local Thomas-Fermi approximation are in reasonable agreement with the results obtained with realistic spectral functions evaluated within the orthogonal correlated basis approach [19,20] unless the calculations are performed for the production of particles at energies substantially below the threshold in free space.

Figure 5 shows that the calculations based on eq. (2) substantially underestimate the data at low masses. This discrepancy can be attributed to the rescattering of the protons after the $K^+n \to K^0p$ reaction in the nuclear medium.

The elastic $pN \to pN$ cross-section on a bound nucleon is evaluated by

$$\frac{\mathrm{d}^3\sigma}{\mathrm{d}p\mathrm{d}\Omega} = \int\Phi(p_p)\mathrm{d}p_p\int P(E_q,q)|T_{NN}(s_{pN},\Omega)|^2\mathrm{d}E_q\mathrm{d}^3q, \quad (7)$$

where $\Phi(p_p)$ is the proton spectrum from the reaction $K^+n \to K^0p$ given by eq. (2) and T_{NN} is the nucleon-nucleon scattering amplitude. The squared invariant energy of the pN interaction is defined analogous to eq. (3).

The relative weight of the $K^+n \to K^0p$ reaction and the proton rescattering contribution is, in principle, related by unitarity, *i.e.* by the total K^+Xe inelastic cross-section. It can be evalulated, *e.g.*, by the formalism given by Glauber [21], Sitenko [22], and Gribov [23]. Based on that formalism one expects that in the case of the Xe nucleus almost 40% of the secondary protons are rescattered. In our calculations the relative weight of the two contributions is treated as free parameter. Because the DIANA results are given without absolute normalization, we normalized the contribution from the direct process by the experimental spectrum at high Kp invariant masses, while the contribution from rescattering is normalized to the low-mass data. The relative weight of direct and secondary contributions resulting from the fit turned out to be 56% and 44%, respectively.

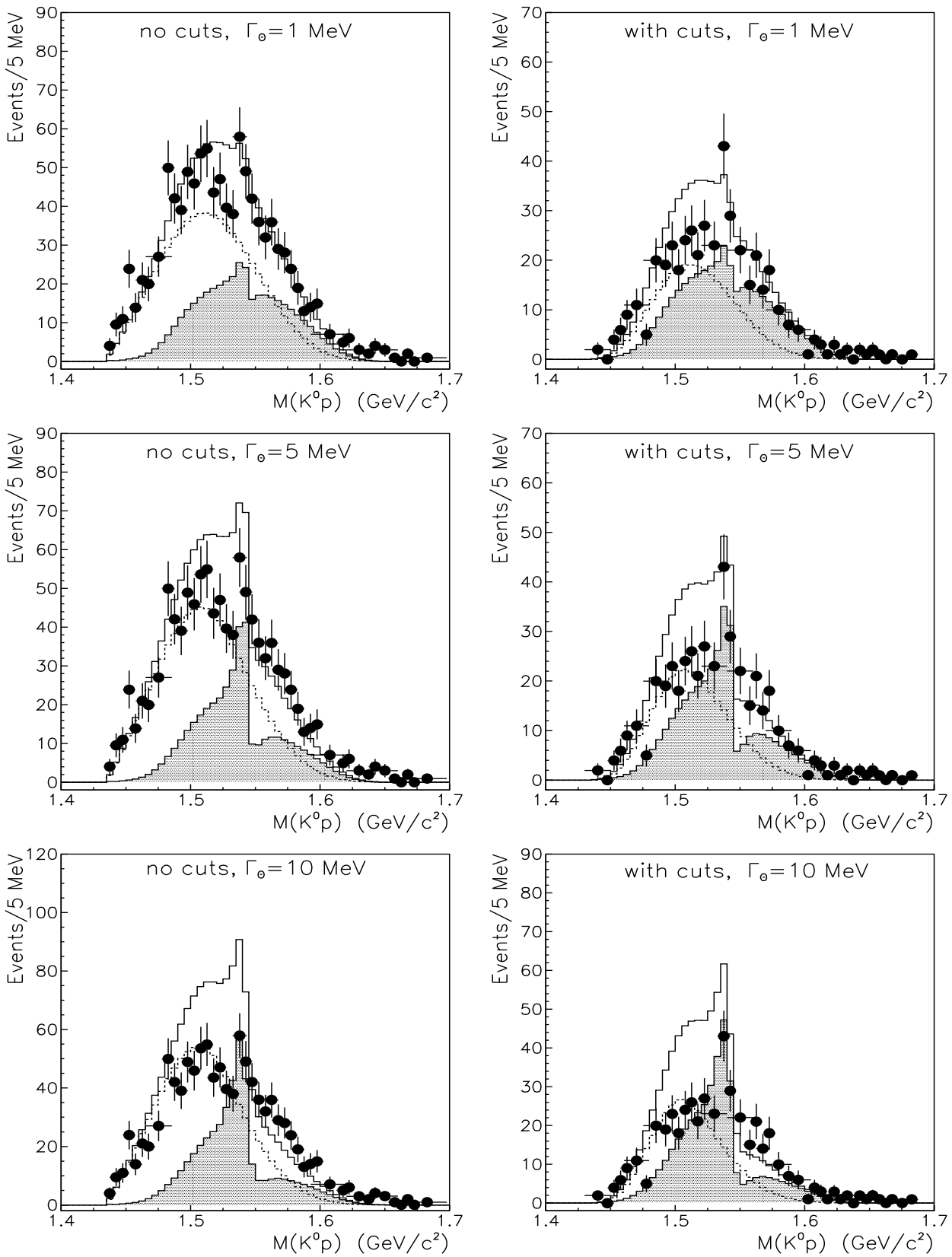

Fig. 6. The same as in fig. 5 but with the inclusion of a Θ^+-resonance with positive parity and a width of 1 MeV (top), 5 MeV (middle) and 10 MeV (bottom). The results are shown without and with kinematical cuts.

The dashed histograms in fig. 5 show the K^0p invariant-mass spectrum calculated with taking into account the rescattering of the proton after the direct $K^+n \to K^0p$ reaction. This spectrum reproduces the shape of the experimental results at low K^0p invariant mass rather well. The sum of the direct and rescattering processes is shown by the solid histograms in fig. 5 and is evidently in quite good agreement with the DIANA data before cuts are made.

The cuts introduced by the DIANA Collaboration aim at a reduction of those events that result from rescattering of the proton. To be specific, only those events are kept that fulfil the critera [2] i) $\theta_p < 100^\circ$ and $\theta_K < 100^\circ$ for the proton and K^0 emission angles with respect to the K^+ direction in the laboratory frame and ii) $\cos\Phi_{pK} < 0$ for the azimuthal angle between the proton and K^0 directions (*i.e.* the proton and K^0 are required to be back-to-back in the plane transverse to the beam direction). When implementing those cuts in our model calculations we keep the normalization of the amplitudes as fixed from the data without cuts. The results are shown in the lower part of fig. 5. They confirm that the goal of those experimental cuts to reduce the background caused by rescattering of the final particles in the nuclear medium is indeed achieved by the cuts. Furthermore, the results illustrate that the kinematical cuts do not introduce any (narrow) enhancement into the K^0p invariant-mass spectrum.

4 Discussion of the Θ^+

The next step is to scrutinize whether the enhancement at the K^0p mass of around $M(K^0p) = 1539\pm2$ MeV is indeed caused by the Θ^+-resonance contribution, which in our calculations enters via the $K^+n \to K^0p$ amplitude. For that we evaluate the K^0p invariant-mass spectra for the reaction $K^+\mathrm{Xe} \to K^0pX$ employing different widths of the Θ^+-resonance and considering positive as well as negative parity for the Θ^+. We always compare our results with the experimental information without and with kinematical cuts. In these calculations we use the same normalization to the data as adopted earlier in the considerations without the Θ^+ contribution.

Figure 6 shows the results for the Θ^+-resonance with positive parity and for a width of 1 MeV (top), 5 MeV (middle), and 10 MeV (bottom), in order. The contribution from the direct $K^+n \to K^0p$ process is shown by the shaded histogram. It clearly reflects the particular bump-dip structure of the elementary KN amplitude that we discussed in sect. 2. Following the experimental analysis we use a binning of 5 MeV for the K^0p mass spectrum, *i.e.* the result of the calculation is integrated over an interval of 5 MeV.

Evidently, the model results for a width of 1 MeV —and without kinematical cuts— are in rather good agreement with the experimental data. In the calculations for a Θ^+ width of 5 MeV (middle panels of fig. 6) the structure from the Θ^+-resonance contribution becomes more pronounced. However, at the same time the data below the resonance region are somewhat overestimated whereas those for higher energies are slightly underestimated. With regard to the data after the kinematical cuts the model results overshoot the experiments already for the original KN model and the situation worsens with inclusion of a Θ^+-resonance and with increasing width.

Table 1. χ^2/d.o.f. evaluated by comparing our calculations for different parity $\pi(\Theta^+)$ and for different Θ^+ widths Γ_{Θ^+} with the experimental information on the K^0p effective-mass spectrum for the reaction $K^+\mathrm{Xe} \to K^0pX$ from the DIANA Collaboration [2]. Considered are the data before the kinematical cuts (44 experimental points) as well as those where cuts were applied (39 points). The first line is the result without inclusion of a Θ^+-resonance.

$\pi(\Theta^+)$	Γ_{Θ^+} (MeV)	No cuts	With cuts
no	no	1.2	2.3
+	1	1.4	2.7
+	5	3.0	3.9
+	10	6.7	7.4
−	1	1.4	2.9
−	5	3.6	5.2
−	10	9.2	11.2

The bottom panels of fig. 6 present our results obtained for a Θ^+-resonance width of 10 MeV. Now there is strong disagreement between our calculations and the DIANA experiment in both cases. For example, after the kinematical cuts the enhancement due to the Θ^+ contribution overestimates the measured signal by a factor of about 1.6. Moreover, the predictions at low masses, *i.e.* below 1539 MeV, significantly overestimate the measurements. Clearly the DIANA data do not support such a large width of the Θ^+-resonance. Note that the width of 10 MeV corresponds roughly to the upper limit for the Θ^+ width of 9 MeV that was claimed by the DIANA Collaboration [2].

Results for the Θ^+ assuming negative parity and again for widths of 1 MeV, 5 MeV, and 10 MeV are presented in fig. 7. Qualitatively the description of the DIANA data is very similar to the case of positive parity. Specifically, there is no obvious evidence that the data favour a particular parity of the Θ^+.

In order to enable an easy quantitative comparison of the various scenarios considered we provide here also the corresponding χ^2 values per data point, cf. table 1. The good agreement of the model calculation based on the original KN model of the Jülich group, without a Θ^+-resonance, with the DIANA data before the kinematical cuts is reflected in the excellent χ^2/d.o.f. of 1.2.

Adding a Θ^+-resonance causes an increase rather than a decrease in the χ^2 value for all considered scenarios, cf. table 1. This increase is clearly marginal for a Θ^+ with a width of 1 MeV, but one would have certainly expected an improvement in the χ^2 once the structure seen in the DIANA data is taken into account in the model calculation. Looking at the DIANA results one can understand what happens. The interpretation of the data as a signal for a narrow structure (*i.e.* the Θ^+) requires also that one takes the dip to the left of the structure seriously. However,

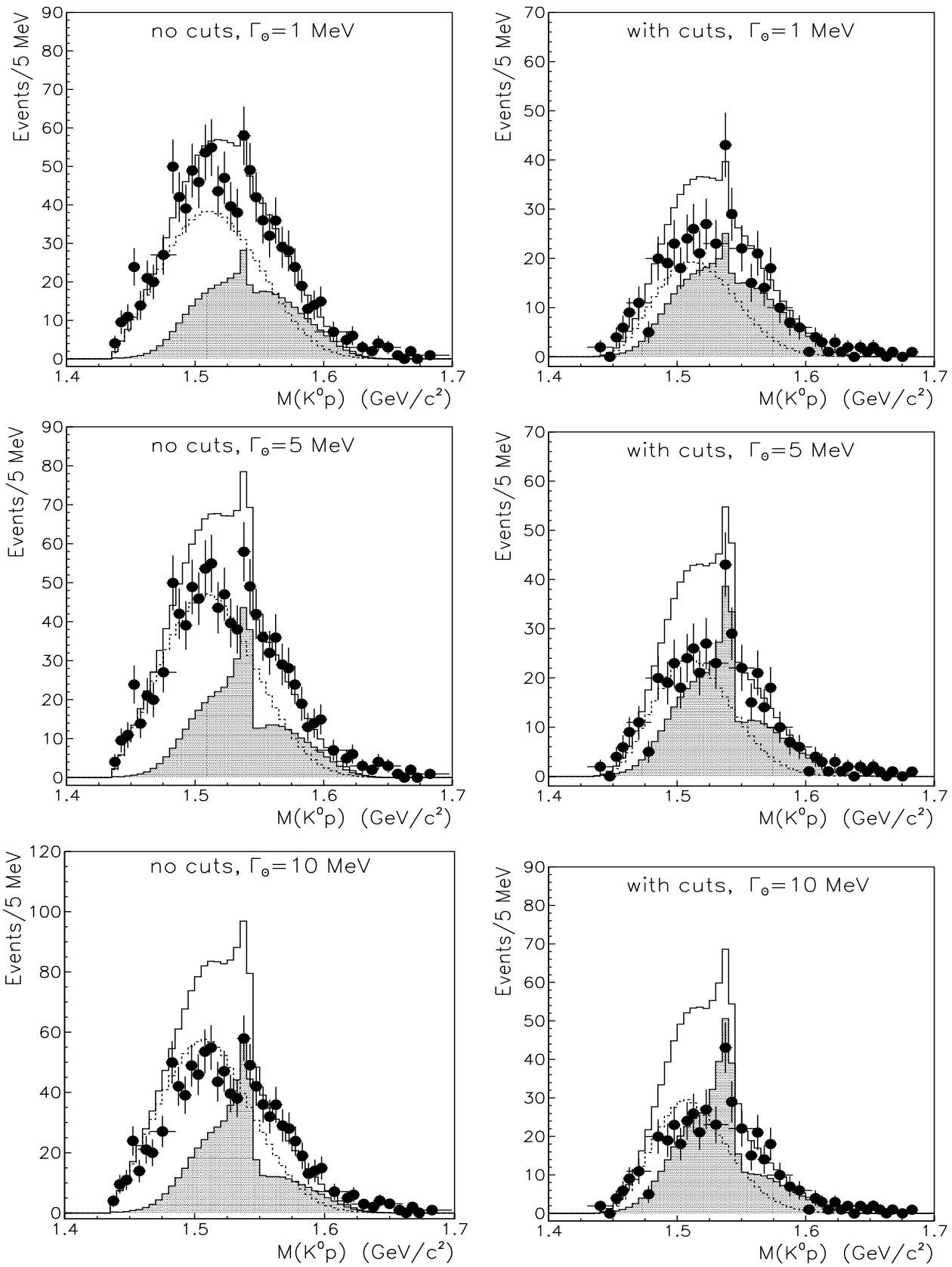

Fig. 7. The same as in fig. 5 but with the inclusion of a Θ^+-resonance with negative parity and a width of 1 MeV (top), 5 MeV (middle) and 10 MeV (bottom). The results are shown without and with kinematical cuts.

such a sharp dip-peak structure can never be produced in a microscopic calculation based on a realistic KN amplitude because the background part of this amplitude is strongly constrained by the KN data and an added resonance structure can only interfere in a particular way with the background as discussed in sect. 2. Since the signal of the actual resonance is strongly reduced compared to the elementary KN cross-section (cf. figs. 5, 6 with fig. 2), specifically for a narrow width, because the calculated results are averaged over bins of 5 MeV —as is done in the experiment— it is not possible to generate a narrow resonance structure and a close-by narrow dip to the left side. This is the reason why the χ^2 does not improve even if a narrow resonance is considered.

For larger widths the data around the maximum of the spectrum are significantly overestimated. Moreover, the dip that develops to the right side of the resonance structure, and which likewise is a consequence of the consistent treatment of the background and resonance part of the elementary KN amplitude in our calculation, becomes more pronounced and causes a further increase in the χ^2/d.o.f. The overall χ^2 deteriorates noticeably for the data with kinematical cuts, cf. the last column in table 1. However, the trend of the χ^2 when adding the Θ^+-resonance is the same as for the data without cuts. As an exercise we also looked at the situation when normalizing the calculations to the data after the cuts. Then it is possible to describe those data with a χ^2/d.o.f. $= 1.4$. (Of course, in this case the corresponding results before the cut deviate more strongly from the data of the DIANA experiments!) But again the χ^2 increases when adding the Θ^+-resonance. Thus, it is clear that the conclusions from our calculation do not depend on whether we normalize to the data before or after the cuts.

5 Summary

We have performed a detailed and microscopic calculation of the K^0p effective-mass spectrum for the charge-exchange reaction $K^+\mathrm{Xe} \to K^0pX$. An enhancement in this quantity at an effective mass close to 1540 MeV, found by the DIANA Collaboration [2], constitutes one of the evidences for the existence of an exotic $S = 1$ (Θ^+) baryon resonance.

The main ingredient of our calculation is an elementary KN scattering amplitude that is taken from the meson-exchange model developed by the Jülich group [3,4]. The role and significance of the Θ^+ for a quantitative description of the DIANA data are investigated by employing variants of the Jülich KN model that include a $\Theta^+(1540)$ resonance, assuming spin 1/2. We considered positive as well as negative parity for the Θ^+-resonance and also a range of values for the width of the resonance.

Since the DIANA Collaboration published results of the measured K^0p mass spectrum prior and after kinematical cuts we could simulate the cuts in our calculation and, specifically, we could compare to the data with and without kinematical cuts in order to control the contribution from the direct $K^+n \to K^0p$ reaction in the Xe nucleus and the rescattering processes. Thereby we could confirm that the broader structure seen in their "raw" data around the effective mass of 1500 MeV is indeed largely due to rescattering processes of the proton after the direct reaction $K^+n \to K^0p$. We also see that the kinematical cuts applied by the DIANA Collaboration do not introduce any (narrow) enhancement in our model results for the K^0p invariant-mass spectrum.

We found that the $K^+\mathrm{Xe} \to K^0pX$ calculations without Θ^+ contribution as well as the results obtained with a Θ^+ width of 1 MeV are in comparably good agreement with the DIANA results. Any spin-(1/2) resonance with a larger width can definitely be excluded. But we must say that even a very narrow structure is only marginally supported by the data. In the light of our results, the high rating of the Θ^+-resonance in the newest version of the PDG tables [24] appears too optimistic. It is evident that more dedicated experiments, employing both strong (*e.g.* at COSY-TOF) and electromagnetic probes, are mandatory to establish this exotic state.

We would like to thank A.G. Dolgolenko for useful discussions.

References

1. T. Nakano *et al.*, Phys. Rev. Lett. **91**, 012002 (2003).
2. V.V. Barmin *et al.*, Phys. At. Nucl. **66**, 1715 (2003), hep-ex/0304040.
3. R. Büttgen, K. Holinde, A. Müller–Groeling, J. Speth, P. Wyborny, Nucl. Phys. A **506**, 586 (1990).
4. M. Hoffmann, J.W. Durso, K. Holinde, B.C. Pearce, J. Speth, Nucl. Phys. A **593**, 341 (1995).
5. J. Haidenbauer, G. Krein, Phys. Rev. C **68**, 052201 (2003).
6. A. Sibirtsev, J. Haidenbauer, S. Krewald, Ulf-G. Meißner, Phys. Lett. B **599**, 230 (2004).
7. R. Machleidt, K. Holinde, Ch. Elster, Phys. Rep. **149**, 1 (1987).
8. B. Holzenkamp, K. Holinde, J. Speth, Nucl. Phys. A **500**, 485 (1989).
9. T. Bowen *et al.*, Phys. Rev. D **2**, 2599 (1970).
10. R.L. Cool *et al.*, Phys. Rev. D **1**, 1887 (1970).
11. A.S. Carroll *et al.*, Phys. Lett. B **45**, 531 (1973).
12. T. Bowen *et al.*, Phys. Rev. D **7**, 22 (1973).
13. C. Gale, G. Bertsch, S. Das Gupta, Phys. Rev. C **35**, 1666 (1987).
14. G.M. Welke *et al.*, Phys. Rev. C **38**, 2101 (1988).
15. S. Frullani, J. Mougey, Adv. Nucl. Phys. **14**, 1 (1984).
16. C. Ciofi degli Atti, S. Simula, Phys. Rev. C **53**, 1689 (1996).
17. A. Sibirtsev, W. Cassing, U. Mosel, Z. Phys. A **358**, 357 (1997).
18. A. Sibirtsev, W. Cassing, U. Mosel, Nucl. Phys. A **679**, 497 (2001).
19. O. Benhar, A. Fabrocini, S. Fantoni, Nucl. Phys. A **505**, 267 (1989).
20. I. Sick, S. Fantoni, A. Fabrocini, O. Benhar, Phys. Lett. B **323**, 267 (1994).
21. R.J. Glauber, G. Mattia, Nucl. Phys. **B21**, 135 (1970).
22. A.G. Sitenko, *Lectures in Scattering Theory* (Pergamon Press Ltd., Oxford, 1971)
23. V.N. Gribov, Sov. Phys. JETP **29**, 483 (1969).
24. Particle Data Group, Phys. Lett. B **592**, 1 (2004).